The ROYAL COLLEGE of
OPHTHALMOLOGISTS

REVIEW ARTICLE

Current and novel multi-imaging modalities to assess retinal oxygenation and blood flow

Michael J. Marino[1] · Peter L. Gehlbach[2] · Abhishek Rege[3] · Kim Jiramongkolchai[4]

Abstract

Retinal ischemia characterizes the underlying pathology in a multitude of retinal diseases that can ultimately lead to vision loss. A variety of novel imaging modalities have been developed to characterize retinal ischemia by measuring retinal oxygenation and blood flow in-vivo. These technologies offer valuable insight into the earliest pathophysiologic changes within the retina and provide physicians and researchers with new diagnostic and monitoring capabilities. Future retinal imaging technologies with the capability to provide affordable, noninvasive, and comprehensive data on oxygen saturation, vasculature, and blood flow mechanics are needed. This review will highlight current and future trends in multimodal imaging to assess retinal blood flow and oxygenation.

Introduction

Retinal hypoxia is implicated in a multitude of prevalent retinal diseases that are potentially blinding. Impaired retinal blood flow (RBF) and/or poor oxygenation are the unifying factors that lead to the blinding complications seen in the microvascular occlusive diseases (retinal artery and vein occlusions) [1–4], diabetic retinopathy [5–8], retinopathy of prematurity [9], sickle cell retinopathy [10], and glaucoma [11–13]. Because RBF and oxygenation are physiological indicators of retinal ischemia that may often precede the appearance of anatomical symptoms such as microaneurysms or thinning of the nerve fiber layer, they are early biomarker candidates for disease diagnostics.

These authors contributed equally: M.J. Marino, P.L. Gehlbach, A. Rege, K. Jiramongkolchai

✉ Kim Jiramongkolchai
  jiramong@gmail.com

[1] Department of Medicine, MedStar Union Memorial Hospital, Baltimore, MD, USA

[2] Retina Division, The Wilmer Eye Institute, Johns Hopkins University School of Medicine, Baltimore, MD, USA

[3] Vasoptic Medical, Inc., Baltimore, MD, USA

[4] Mid-Atlantic Kaiser Permanente, McLean, VA, USA

Monitoring these parameters may also be useful in the surgical setting. Prolonged interventional procedures such as vitreoretinal surgery may also subject the retina and optic nerve to extended periods of ischemia potentially resulting in long-term complications, secondary glaucoma, and visual loss [14, 15]. Hayreh et al. have shown that retinal damage is irreversible after 97 min of central retinal artery occlusion (CRAO) [16]. Oz et al. have shown (in animal models) that transient ischemia over shorter 5–10 min periods also induce retinal degeneration [17]. In particular, patients with diabetic retinopathy (DR) experience significantly decreased ocular blood flow following vitrectomy [18, 19], which may contribute to the variable functional outcome reported with vitrectomy [20–24]. Currently, the gold standard for measuring retinal perfusion involves injecting a fluorescent dye intravenously and then imaging the retina. As the dye fills the vessels, it reveals the anatomical pattern of blood vessels and demonstrates their filling patterns. Other available methods to demonstrate retinal blood flow include intraocular probes, laser doppler flowmetry, laser speckle contrast imaging, retinal oximetry, and an adaptation of optical coherence tomography (OCT) called OCT angiography (OCTA). Because of widespread recognition of the value of assessing the perfusion status of the retina, there is significant research development activity seeking to improve the reliability and usability of imaging technologies. There is now increasing interest in developing in-vivo imaging techniques to study oxygen metabolism in the retina.

This is in part due to the fact that a number of diseases result from a complex interaction of more than one systemic pathology. Therefore, disease management can benefit from an integrated approach to information processing [25]. For example, the retina is an embryologic derivative of the brain that retains direct anatomical connections. Assessment of vascular status in the retina is now known to provide information regarding the vascular status in the brain [26–28], thus providing insights into conditions with neurovascular symptoms/aetiologies such as stroke [4, 29, 30], the vascular dementias, and cognitive decline [31]. The eye also represents an avenue to probe small caliber vessels noninvasively for insights into overall vascular and cardiovascular health [32–34]. The only other exposed/directly accessible small caliber vessels are in the skin where the circulation has multiple redundancies and is particularly sensitive to highly variable factors such as temperature and contact/pressure. Surrogacy of ophthalmic imaging is therefore gaining prominence as a window into systemic cardiovascular health [35, 36], and neurovascular health [26, 27]. At the present time correlations between retinal vascular status and the incidence of stroke have been shown [29, 37], as have correlations between retinal perfusion and the stage of Alzheimer's disease [38, 39].

In this review, we aim to discuss the physiology underlying the distribution and consumption of oxygen in the retina as well as examine the presently available techniques, both invasive and noninvasive, that are used to study retinal blood flow and oxygenation.

Background

The retina is a multilayered heterocellular organ that lines the interior of the globe with predominantly neural elements that are derived from the brain during development. The retina is responsible for capturing and converting light energy into neural impulses that travel down the optic nerve axons to the brain's visual cortex for processing to produce visual images that are eventually interpreted by the frontal cortex. This complex biochemical process requires a vast amount of cellular energy, which is primarily derived from oxidative metabolism coupled to ATP synthesis. Oxygen consumption in the retina (on a per gram basis) exceeds that of the brain and is the most metabolically active tissue in the body [40, 41]. Such a high metabolic demand necessitates a robust blood supply in order to provide for tissue oxygenation and removal of metabolic by-products [42].

The primary blood supply to the eye is the ophthalmic artery, a branch of the internal carotid artery. The ophthalmic artery gives rise to the ciliary arteries and the central retinal artery. The posterior ciliary arteries supply the choroid. Oxygen-rich blood is able to diffuse from the smallest choroidal vessels, termed choriocapillaries, through Bruch's membrane and the retinal pigment epithelium to eventually reach the layer of photoreceptors in the outer retina [3]. The human retina receives oxygenation from two sources. The outer layer of the retina, which contains the outer segments of the rods and cones, is nourished by the choroidal vessels. The central retinal artery in turn supplies the inner retina [3]. The oxygen diffusion process described above is driven by a high concentration gradient for oxygen and overlaps the mid-retina [43]. The overlapping region in the retina where oxygen from both the choroidal vessels and the retinal arterioles is present represents an oxygen watershed zone. Therefore, blood flow and oxygenation in different regions of the posterior segment may offer clues to different conditions. For example, conditions like retinopathy of prematurity and diabetic retinopathy are known to exhibit pathology in the peripheral retina first [44], while assessment of glaucoma could benefit from and assessment of perfusion of the optic nerve head and the retinal ganglion cells [45].

Current methods

Dye-based angiography

The historical and present gold standard method for imaging the retinal circulation is fluorescein angiography (FA). Fluorescein sodium is a fluorophore with a long history of being used in ophthalmology, having been reported in the literature as early as 1930 [46]. This technique involves injecting a fluorescein dye solution intravenously and then taking sequential timed images of the retina [47]. The movement of the dye through the vasculature over time can reveal characteristic patterns (ex: dye leakage, pooling, dropout, and staining) consistent with normal or impaired retinal circulation.

Although at present FA remains the gold standard, it does not provide excellent visualization of all of the retinal capillaries and it fails to differentiate fluorescence from overlapping structures. When combined with ultra wide field imaging using instruments such as the Optomap (Optos PLC, Marlborough, MA) it becomes possible to observe leakage in the peripheral retina facilitating disease management prior to the development macular pathology [48]. The deeper capillary networks of the retina, especially

Fig. 1 **Optic nerve head and peripapillary vascular network.** This image depicts a fluoroscein angiographic image (**A**) and optical coherence tomography angiography image (**B**) in the same region of the right eye. Note the increased definition of the radial peripapillary capillary network in image B. This image was reproduced with permission from Spaide et al. (2015) [46].
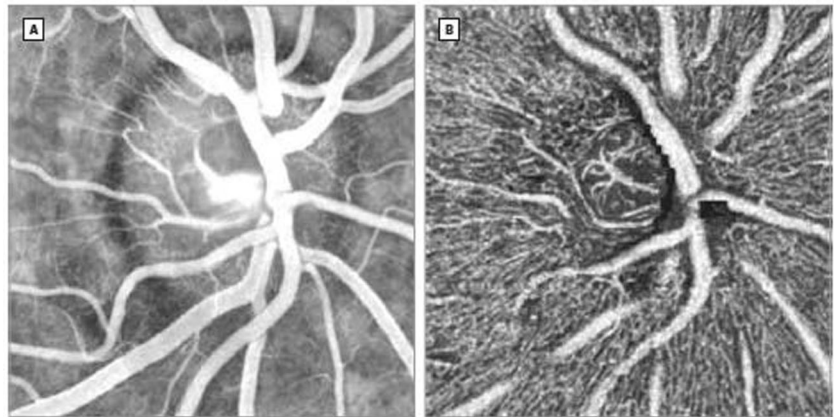
the radial peripapillary capillaries, are not visualized well by FA (Fig. 1) [49]. This is due to the more rapid leakage of fluorescein from fenestrated choriocapillaries, which obscures deeper choroidal vessels [50]. Furthermore, FA has been reported to be associated with potential adverse effects such as nausea, vomiting, pruritis, cardiac arrest, clonic seizures, and even death [51–53].

Indocyanine green dye (ICG) can also be used for retinal angiography. Since being approved for clinical use in 1956, ICG has been used for over 30 years systemically to cardiac output and hepatic function and blood flow [54–56]. This dye allows for better penetration of fluorescence through the retinal pigment epithelium resulting in better delineation on images of the choroidal vessels [50]. ICG does not diffuse through the choriocapillaries as rapidly as fluorescein as it is ~98% bound to plasma proteins. This compares to fluorescein which is 60–80% bound to intravascular plasma proteins [50]. Unlike fluorescein, ICG is cleared exclusively by the liver. ICG is not as widely used as FA but systemic reviews suggest it may have a better tolerability and safety profile. While the incidence of mild and moderate adverse reactions to fluorescein angiography is 1–10% [53] and 1.6%, respectively, the rate of mild adverse reaction to ICG is reported to be as low as 0.15% [57] and 0.2% [57], respectively. The incidence of death from anaphylaxis following injection of fluorescein injection is higher than ICG. The rate of death after injection of fluorescein angiography is reported to be 1:222,000 while the rate of death after ICG injection is 1:333,333 [53, 57]. ICG is associated with adverse reactions in patients with uremia and liver disease. Use of ICG in pregnant women is controversial. ICG contains iodine and should not be administered to patients with definite iodine allergy.

A variation on FA involves injecting an oxygen-sensitive dye into the blood stream. The dye is then illuminated with light of a certain wavelength and the detected light provides information on the oxygen concentration in the vicinity of the dye [58, 59]. Unfortunately, this technique is only useful for animal studies as the oxygen-sensitive dye is not considered safe for human use.

OCT angiography

Another noninvasive approach to angiography, optical coherence tomography angiography (OCTA), is a relatively new imaging modality that involves acquiring consecutive transverse cross-sectional optical coherence tomography (OCT) scans and attributing the differences in the scans to flowing blood. Thus, a map of perfused microvasculature is constructed based on analyzing the decorrelation between the two OCT data sets (Fig. 2) [60]. Due to its lack of reliance on exogenous contrast agents, OCTA is rapid, safe, and convenient, and its increasing adoption has contributed to the growing recognition of the value of perfusion assessment in the clinic [12, 61]. OCTA has been reported to have excellent spatial resolution as it can produce revealing visualizations of perfused microvasculature down to the capillary level, permitting assessment of features such as the foveal avascular zone (FAZ), the size of which has been measured and correlated with disease status [62–66]. The quest for developing quantitative metrics from OCTA data that is useful as biomarkers for clinical disease has led to the development and validation of automated means of estimating vessel density or perfusion density, as well as the area of the FAZ. Perfused vessel density measurements have been shown to exhibit a mean coefficient of variation (CV) of 6.72% by Lee et al [67], while Al-Sheikh et al. report a CV of 5.2% for superficial retinal layers and 2.0% for deeper retinal layers [68]. Inter-visit repeatability of OCTA measurements in the optic nerve head region is also high (CV < 5.2%) as reported by Chen et al. [69]. Intra-subject repeatability of automatically estimated FAZ area has been reported to be high, as inferred from a mean CV less than 2.66% across two operators, and ICC greater than 0.958 (0.905–0.982) across three devices [70]. OCTA and OCTA-derived metrics do however have some significant
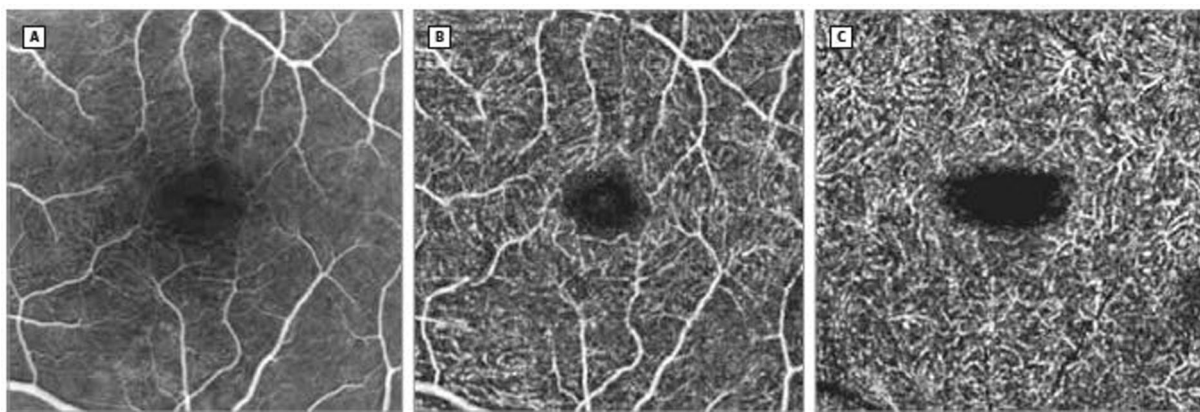
Fig. 2 Comparison between a fluorescein angiographic image and OCTA images of the Macula. This image depicts a fluorescein angiographic image of the central macular region (**A**), OCTA image of the inner retinal vascular plexus (**B**), and OCTA image of the outer plexus (**C**). This image was reproduced with permission from Spaide et al. (2015) [46].

limitations. Vessel density is not a scale invariant metric, susceptible to confounding effects of vessel diameter. The duration of image acquisition makes OCTA susceptible to motion artifacts [49], and limits its temporal resolution, which also implies that output perfusion data is aggregated over the pulsatile rise and fall of blood flow within a cardiac cycle. High-speed OCTA using a swept source has resolved blood flow fluctuations through averaging over an extended period of time [71]. Other advances in OCT angiography include prototypes that enable use in a handheld configuration [72, 73].

Probes

Oxygen-sensitive probes can be inserted into the vitreous cavity and gather information from directly above the retina, or even penetrate the retina [3]. Preretinal measurements of the partial pressure of oxygen are thought to represent the oxygenation status of the inner retina [74, 75]. This is because the vitreous body has no blood vessels and normally has a low level of oxygen consumption [74]. Therefore, the partial pressure of oxygen (PO_2) in the vitreous body is primarily determined by the PO_2 in the surrounding tissues. Studies have shown that the PO_2 is highest in areas closest to the retina and lowest in central parts of the vitreous closest to the lens [74]. This oxygenation distribution infers that oxygen not consumed by the retina diffuses from the retina toward the lens. Thus, the PO_2 in the area of the vitreous closest to the retina depends mainly on the mean PO_2 in the innermost layer of the inner retina [74]. The two types of probes in use today include one containing an oxygen-sensitive polarographic electrode and another containing an oxygen-sensitive dye.

The oxygen-sensitive dye is traditionally composed of a metalloporphyrin (ex: palladium-mesotetra-(4-carboxyphenyl)-porphyrin) [3]. Notably, this dye is distinct from the unsafe injected dye mentioned in the angiography section above. When the tissue of interest is illuminated, light is absorbed by the dye exciting its electrons into the triplet state. Electrons in the triplet state then return to the ground state either by light emission or by transferring the energy to other molecules in a process called quenching. In vivo, the primary quenching agent is oxygen [76]. The molecular interaction between the quencher (oxygen) and the luminophore (porphyrin dye) is termed collisional quenching and the quenching rate is diffusion limited [77]. Although the mechanism by which oxygen quenches luminescence is not completely understood, one hypothesis suggests that the oxygen causes the luminophore to cross into the triplet state while molecular oxygen goes to the excited state and then returns to the ground state [78]. The result of this interaction is the formation of singlet oxygen ($^1O_2$), which demonstrates that energy transfer has occurred [77]. In addition, the quenching mechanism can happen through the transfer of electrons [77]. Regardless of the mechanism of collisional quenching, the kinetics of this reaction can be described by the Stern-Volmer equation:

$$\frac{I_0}{I} = \frac{\tau_0}{\tau} = 1 + k_q \tau_0 pO_2 = 1 + K_{sv} pO_2$$

In this equation, I and I_0 are the luminescence intensities in the presence and absence of the quencher, τ and τ_0 are the lifetimes of the luminophore in the presence and absence of the quencher, k_q is the biomolecular quenching constant, and K_{sv} is the Stern-Volmer quenching constant [77]. The Stern-Volmer relation can be used to calculate the concentration of oxygen from the intensity of the emitted light or from the lifetime of the triplet state [76].

The electrode-tipped probe gathers data through an electrochemical reaction that requires oxygen as a substrate. This oxidation-reduction (redox) reaction can be described by the following: $O_2 + 2H_2O + 4e^- \rightarrow$

$4OH^-$ and $4Ag + 4Cl^- \rightarrow AgCl + 4e^-$ which take place at the probe's cathode and anode, respectively. It is important to note that this equation represents the reaction that takes place at the silver reference wire as described by Stefansson et al in 2005 [75]. Probes tipped with other elements will exhibit different redox reactions. The rate of the reaction depends on the concentration of dissolved oxygen in the area surrounding the probe. The electrode measures a current and this current can then be correlated to a certain oxygen concentration [3]. This technique requires the electrode to be calibrated in solutions of known PO_2 levels. There is a linear relationship between the electrode current and the measured PO_2 for PO_2 values between 0 and 200 mm Hg [74]. The current is produced by the electrochemical reduction of oxygen at the active surface of the electrode [74].

The downside to using probes is that their size restricts to use in patients who are undergoing vitrectomy. To obtain oxygen measurements intraoperatively, the probe needs to be calibrated in a balanced salt solution before each set of measurements is taken [79, 80]. Then the probe is introduced into the vitreous cavity. The oxygen measurements are obtained by holding the probe in place until constant values are recorded. Measurements are often taken in the mid-vitreous cavity and pre-retinal vitreous [80]. The vitreous is avascular and acts as a diffusion medium with little to no oxygen consumption [75]. Therefore, the oxygen tension in the vitreous body represents the oxygen consumption in the surrounding tissues. Importantly, it is not possible to position the probe directly behind the lens capsule in patients with phakic eyes due to the risk of lens damage [79].

Noninvasive laser-based imaging

Laser Doppler Velocimetry (LDV), also called laser doppler flowmetry, is a noninvasive method used to measure the blood speed in retinal vessels using the Doppler effect [81]. Laser light incident on and returning from a moving particle experiences a shift in frequency that is proportional to the velocity of the moving particle [82], and can be measured using interferometric means. While LDV can produce images of retinal blood speeds with a high temporal resolution [83, 84], its spatial resolution is limited by the resolution of interferometric detectors. A severe limitation of LDV has been its poor repeatability of measurements with CV ranging from 4.8 to 39.7% (median 19.9%) [85]. Doppler-based assessment of ocular blood speeds has been most effectively used in combination with OCT (Doppler OCT) [86–88] or ultrasound called Colour Doppler Imaging or CDI [89–91] wherein the Doppler signal depicted in pseudo-colour is overlaid on the available structural data. Because the Doppler-based frequency shift depends on the relative orientation of the moving particle and the path of light, a three beam configuration has been developed to simultaneously eliminate this dependence and obtain the blood velocity vector as opposed to just the blood speed [86].

The authors have personal experience in developing and applying laser speckle contrast imaging (LSCI). LSCI is a noninvasive wide field optical imaging scheme that leverages a different phenomenon associated with high-coherence lasers, namely speckle production [92]. When the retina is photographed under laser illumination, erythrocyte motion causes a blurring effect in the speckle pattern at the camera sensor [93]. Such blurring effect can be computationally analyzed to infer the rate of blood motion by computing a parameter called speckle contrast, defined at a location as the CV of pixel intensities in the location's spatio-temporal surroundings [94, 95]. Spatio-temporal surroundings refers to pixels in a spatial window around the location within the same image frame or in adjacent image frames acquired sequentially [96]. Therefore, LSCI also reveals perfused blood vessels with high contrast because of the differences in orderly vascular blood flow and the lack thereof in non-vascular tissue [97]. LSCI has been used to image ophthalmic circulation since 1982 [98], and an instrument called LSFG-NAVI (Softcare Co. Ltd., Fukuoka, Japan) has been extensively used to assess the role of LSCI-based mean blur rate in healthy and diseased eyes [1, 99–101]. Recently, a new instrument called the XyCAM RI (Vasoptic Medical, Inc., Baltimore, MD) developed by (AR) has been introduced that produces reliable measurements of blood flow velocity indices (BFVi) within a circular field of view of 25 degrees with a superior temporal resolution of 82 frames/second for up to 6 seconds [102]. In the authors experience, repeatability and reproducibility of BFVi measurements has been reported to be high in vessel segments, foveal region, and standard regions around the fovea [103]. The high temporal resolution facilitates visualization and analysis of RBF dynamics as it fluctuates between a dip and peak value corresponding to the diastole and systole of a cardiac cycle (Fig. 3) [104]. LSCI permits differential assessment of blood flow patterns in retinal arteries and veins (Fig. 3) [102, 105–107]. If LSCI data sets of multiple fields of view are acquired rapidly in succession, it also becomes possible to generate reliable wide-field montages of RBF dynamics [108]. LSCI technology is particularly exciting also because the instrumentation is amenable to miniaturization and cost effectiveness [109], and also practical for use in a handheld configuration as has been shown by Rege et al [97]. As a non-scanning full-field technique comprising high speed image acquisition, LSCI permits spatial/regional assessments with low susceptibility to motion artifacts. LSCI utilizes narrow band laser illumination with peak
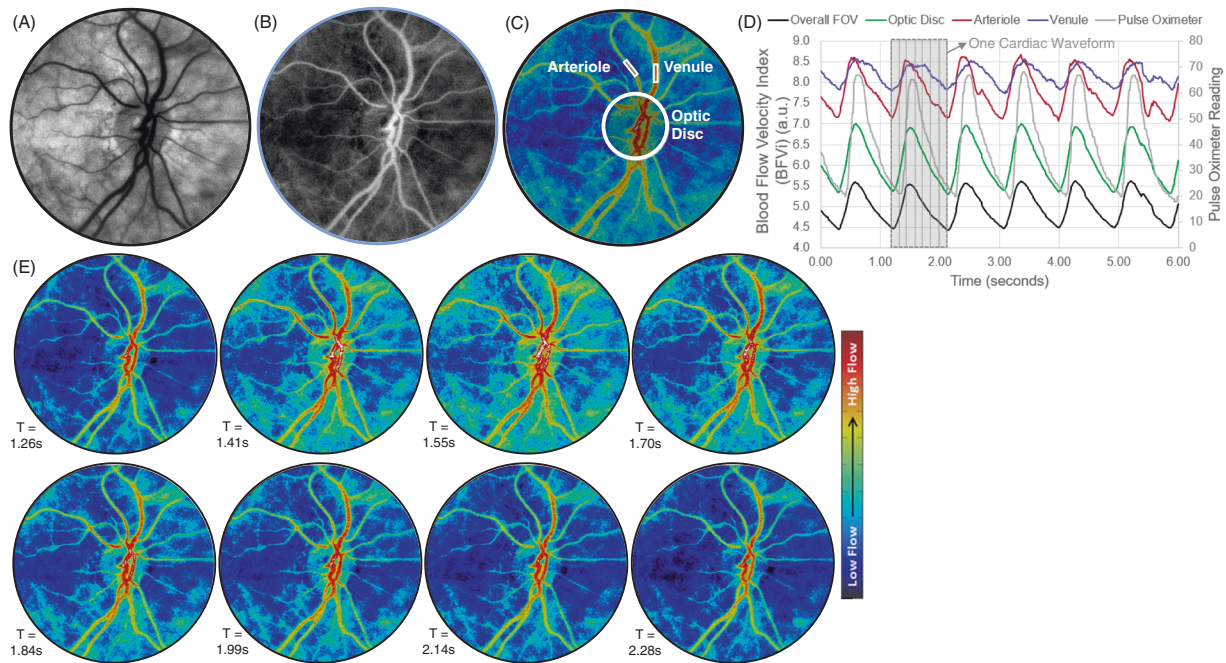
Fig. 3 Imaging of retinal blood flow dynamics with high temporal resolution using laser speckle contrast imaging by the XyCAM RI. The XyCAM RI produces complementary visualization of vessel morphology (**A**), and a dye-free angiogram (**B**). **C, D** The XyCAM RI data obtains blood flow velocity index (BFVi) at a high temporal resolution that can be aggregated over the entire field of view or within custom-defined regions such as optic disc, an arteriolar segment or a venular segment. **E** Eight snapshots of BFVi (depicted in pseudo-colour) at discreet timepoints (indicated by dotted vertical lines in (**D**)) over a single cardiac cycle reveal visually the pulsatile nature of ocular blood flow.

wavelength in the near infrared spectrum which reduces the risk of phototoxicity at the retina and facilitates imaging without pupillary constriction or patient discomfort.

In the authors experience, limitations of LSCI are the following. Use of LSCI is limited to obtaining *en-face* blood flow and as a two-dimensional technique, it is unable to resolve blood flow along the depth dimension. BFVi captures the effect of blood speed as well as blood vessel diameter as information captured by the two-dimensional camera sensor represents blood motion aggregated from the depth of focus. By integrating BFVi along the *en-face* diameter of a vessel, it becomes possible to estimate blood flow rates [110]. Furthermore, LSCI-based outputs (MBR and BFVi) provide estimates of blood flow as opposed to absolute values [111]. However, these estimates are repeatable and reproducible, thus make it possible to compare these values. As in the case of OCTA, normalized metrics available from analysis of the blood flow waveform provide additional comparison metrics [13, 100, 102].

Two techniques have reported in vivo measurements of absolute blood flow in the retina. One is the Retinal Function Imager or RFI (Optical Imaging Ltd., Rehovot, Israel), which computes blood velocity by tracking erythrocytes in a sequence of 8 fundus camera image frames obtained under bright green illumination. Repeatability of RFI measurements has been reported to be good by some investigators while others have found it lacking [112, 113]. In addition to a bulky form factor and a hefty price tag, adoption of RFI in the clinic has been limited possibly because of the discomfort associated with maintaining a steady gaze over almost 125 milliseconds of intense green illumination. The other technique of absolute blood flow measurement is called Erythrocyte Mediated Angiography (EMA) and involves the ex vivo labeling of erythrocytes by a fluorescent dye and their re-introduction into the blood stream for tracking and flow estimation purposes [114, 115]. Automated tracking of fluorescent particles permits a nuanced assessment of velocity and flow and is easier to quantify in capillaries than in larger vessels [116, 117]. While both RFI and EMA directly track erythrocytes and therefore could be contemplated as absolute indicators of velocity, the accuracy of flow measurement depends on the success of tracking algorithms as well as the fractional concentration of erythrocytes detected for tracking among all erythrocytes flowing in the vessel segment at a given time.

Absorption-based techniques for oximetry

Dual wavelength oximetry

Spectrophotometric retinal oximetry provides a noninvasive measurement of oxygen saturation in the retinal vessels.

The principal underlying this technique is based on the difference in the wavelength absorption of oxyhaemoglobin and deoxyhaemoglobin. Conventional techniques used to perform retinal oximetry utilize white light illumination of the fundus with the subsequent image then being split and filtered with light filters for spectrophotometric analysis. Currently there are 2 commercially available systems: OxymapT1 (Oxymap, Reykjavik, Iceland) and the Dynamic Vessel Analyzer (Imedos Systems GmbH, Jena, Germany) [118, 119]. Both commercial units use conventional fundus cameras and dual wavelength analysis. These dual wavelength retinal oximetry systems have been used to study diabetic retinopathy, glaucoma, and retinal vascular occlusion but have not yet entered mainstream practice due to clinical relevance, lack of normative values, and required manual correction [120–122].

Multispectral oximetry analysis Other approaches to retinal oximetry have used multispectral analysis. Traditional digital images produce very limited spectral information registering images as only monochromatic or trichomatic (red, green, blue) light as reflected by the retina structures. Hyperspectral imaging (HSI) overcomes these limitations by capturing information from multiple wavelengths beyond the traditional trichromats and generates a four element hyperdimensional cube: two dimensions for spatial data, a third dimension for wavelength bands, and a fourth dimension that corresponds to the absorbance and reflectance at each wavelength. HSI has the ability to collect information from 10 to hundreds, that is, a continuum of wavelength bands whereas multispectral imaging typically refers to 3–10 discreet bands of wavelengths [123]. The hyperspectral cube analyzes reflected light captured by the spectrometer. HSI collects substantially more information than conventional fundus imaging but its use is considered to be emerging. In the usual set-up, a light source emits light at the retina which is then partly reflected and transmitted from the retina. The reflected or transmitted light is then captured by a detector which is commonly a charge coupled device (CCD). Most cited ex vivo microscopy techniques use the transmittance mode meaning the detector captures light that is transmitted through the retina. In-vivo imaging using reflectance mode meaning the light reflected from the retina surface is captured by the detector. To capture the multiple wavelengths several, bandpass filters designed to allow selected ranges of wavelengths to be transmitted while reflecting others [123]. Bandpass filters such as liquid crystal filters or prism grating prism arrays separate the wavelengths into a "rainbow" of distinctly separated colourcolours. Another approach involves using different wavelengths (ranging from visible to near infrared to specific wavelengths) to illuminate the retina. Despite the differing approaches of illuminating and filtering wavelengths of light, all of these setups share a commonality in the generation of a hyperspectral cube which contains spectral information for each spatial dimension. Oximetry data is calculated by taking the ratio of the optical density (one sensitive to saturation and the other isosbestic) using a formula which removes the incidental outliers [124] or by using the Beer Lambert law for several wavelengths [60].

A recent article by Lemmens et al., describes HIS's application to ophthalmology to be still in early development [123]. There are still significant challenges before his technique can gain wide acceptance. First, HSI setups are not uniform and most clinical case reports represent proof of concept. As a result of lack of uniformity, there is no normative database. Second, HSI contains artifacts that may limit its use: Stokes shift, spatial resolution, and ocular movement.

Multispectral imaging has established applications beyond ophthalmology to other medical fields such as dentistry and histopathology to aerial mapping. An emerging application of MSI is to visualize each layer of the retina. MSI uses light emitting diodes (LED) which contain a broad spectrum of wavelengths to visualize each layer of the retina and the choroid, which requires a longer wavelength [125]. Spectral filters deliberately separate the wavelength of the LED to examine the tissue via differential scatter, reflection, and absorption. The short wavelength of LED is used to study the anterior retinal layers of the retina. This is advantageous when studying the internal limiting membrane layer of the retina which will appear nearly invisible under white light. Medium wavelengths, enable visualization of the mid retina and are especially helpful for identifying hemorrhages, drusen, exudates, and neovascularization. Longer wavelengths, allow visualization of the retinal pigmented epithelium and choroidal structures and clinical characterization of subretinal and intraretinal hemorrhages, photoreceptor loss, choroidal nevi, and choroidal melanoma. The discrete LED and filters of MSI enable visualization of in-vivo layers of the retina that is not possible with traditional monochromatic spectral imaging.

Discussion

Primary retinal diseases as well as systemic diseases known to affect the retinal vasculature such as diabetes can be diagnosed and monitored for progression by assessing the morphology and physiology of the retinal vasculature. At this time, the technologies available to measure retinal blood flow mechanics can be divided into those that are invasive and those that are noninvasive and depend on advanced imaging techniques and lasers. While invasive techniques such as intraocular probes and fluorescein angiography can provide accurate data about retinal oxygenation and the retinal vasculature respectively, their utilization must be

weighed against the potential iatrogenic effects associated with invasive procedures. Noninvasive technologies can be divided into the type of illuminating light used and filters applied. The illuminating light can be utilized to examine specific layers of the retina (inner, middle, outer), The type of filter applied can provide depth resolved tissue analysis and obtain information pertaining to retinal oxygenation. Improvements in each of these technologies are still necessary in order to visualize the anatomy of the entire relevant retinal vasculature, measure blood flow through it, and assess the resulting retinal oxygenation with either one comprehensive technique or the coordination of multiple technologies. Newer technologies that rely on scanning in the spatial or spectral domains have longer data acquisition time which makes these techniques susceptible to artifact generated by normal eye saccades, corneal dryness, outlier post processing artifacts, eventually requiring time-consuming manual review and correction. Larger studies are required to establish a normative database for clinical usefulness. With advances in high-speed computing, global efforts in sharing of large clinical databases, and analytical techniques based on machine learning and other artificial intelligence methods, these limitations are expected to be addressed in the near future.

Conclusion

Retinal tissue is the most metabolically active tissue in the body and requires a constant supply of nutrients and oxygen. Blood flow to the retina can be compromised by a variety of prevalent retinal conditions as well as systemic pathologies. A retina that receives suboptimal perfusion for an extended period is susceptible to irreversible ischemic damage, and even reperfusion following a significant ischemic period can create additional retinal injury. The result is retinal damage that in worst cases leads to permanent blindness. A variety of techniques are currently employed to gather data not only on the anatomy of the retinal vasculature but also on the perfusion dynamics. Each technique yields specific data types and often, multiple techniques are used collaboratively to provide a more detailed picture of retinal blood flow. The ideal imaging technology will have the functionality to measure oxygen saturation, provide dynamic retinal blood flow measurements, and be able to image the entire retinal tissue volume. Technological advances are being made at an unprecedented pace as an affordable, noninvasive view of the architecture of the retinal vessels combined with quantifiable data on both retinal hemodynamics and oxygenation can be an asset not only to an ophthalmologist but eventually to a primary physician for systemic cardiovascular health insights.

Compliance with ethical standards

References

1. Matsumoto M, Suzuma K, Yamada Y, Tsuiki E, Fujikawa A, Kitaoka T. Retinal blood flow levels measured by Laser Speckle Flowgraphy in central retinal vein occlusion as a predictive factor for ischemia and visual loss. Investigative Ophthalmol Vis Sci. 2013;54:5126.
2. Rong AJ, Swaminathan SS, Vanner EA, Parrish RK. Predictors of Neovascular Glaucoma in Central Retinal Vein Occlusion. American Journal of Ophthalmology. 2019;204:62–9.
3. Hardarson SH. Retinal oximetry. Acta ophthalmologica. 2013;91 (Thesis2):1–47.
4. McGeechan K, Liew G, Macaskill P, Irwig L, Klein R, Klein BE, et al. Prediction of incident stroke events based on retinal vessel caliber: a systematic review and individual-participant meta-analysis. American journal of epidemiology. 2009;170:1323–32.
5. Nagaoka T, Sato E, Takahashi A, Yokota H, Sogawa K, Yoshida A. Impaired retinal circulation in patients with type 2 diabetes mellitus: retinal laser Doppler velocimetry study. Investigative Ophthalmol Vis Sci. 2010;51:6729–34.
6. Dirani M, McAuley AK, Maple-Brown L, Kawasaki R, McIntosh RL, Harper CA, et al. Association of retinal vessel calibre with diabetic retinopathy in an urban Australian indigenous population. Clin Exp Ophthalmol. 2010;38:577–82.
7. Cuypers MH, Kasanardjo JS, Polak BC. Retinal blood flow changes in diabetic retinopathy measured with the Heidelberg scanning laser Doppler flowmeter. Graefes Arch Clin Exp Ophthalmol. 2000;238:935–41.
8. Burgansky-Eliash Z, Nelson DA, Bar-Tal OP, Lowenstein A, Grinvald A, Barak A. Reduced retinal blood flow velocity in diabetic retinopathy. Retina. 2010;30:765–73.
9. Ozcan PY, Dogan F, Sonmez K, Con R, Dokumaci DS, Seyhanli ES. Assessment of orbital blood flow velocities in retinopathy of prematurity. Int Ophthalmol. 2017;37:795–9.
10. Abdalla Elsayed MEA, Mura M, Al Dhibi H, Schellini S, Malik R, Kozak I, et al. Sickle cell retinopathy. A focused review. Graefes Arch Clin Exp Ophthalmol. 2019;257:1353–64.
11. Fan N, Wang P, Tang L, Liu X. Ocular Blood Flow and Normal Tension Glaucoma. Biomed Res Int. 2015;2015:308505.
12. Schuman JS. Measuring Blood Flow: So What? JAMA Ophthalmol. 2015;133:1052–3.
13. Shiga Y, Omodaka K, Kunikata H, Ryu M, Yokoyama Y, Tsuda S, et al. Waveform Analysis of Ocular Blood Flow and the Early Detection of Normal Tension Glaucoma. Investigative Ophthalmol Vis Sci. 2013;54:7699–706.

14. Jain N, McCuen BW, Mruthyunjaya P. Unanticipated Vision Loss After Pars Plana Vitrectomy. Survey of Ophthalmology. 2012;57:91–104.

15. Marti M, Walton R, Boni C, Zweifel SA, Stahel M, Barthelmes D. Increased Intraocular Pressure Is a Risk Factor for Unexplained Visual Loss during Silicone Oil Endotamponade. Retina. 2017;37:2334–40.

16. Hayreh SS, Zimmerman MB, Kimura A, Sanon A. Central retinal artery occlusion.: Retinal survival time. Exp Eye Res. 2004;78:723–36.

17. Öz Ö, Gürelik G, Akyürek N, Cinel L, Hondur A. A Short Duration Transient Ischemia Induces Apoptosis in Retinal Layers: An Experimental Study in Rabbits. Eur J Ophthalmol. 2005; 15:233–8.

18. Sharma T, Fong A, Lai TY, Lee V, Das S, Lam D. Surgical treatment for diabetic vitreoretinal diseases: a review. Clin Exp Ophthalmol. 2016;44:340–54.

19. Nakashima H, Iwama Y, Tanioka K, Emi K. Paracentral Acute Middle Maculopathy following Vitrectomy for Proliferative Diabetic Retinopathy: Incidence, Risk Factors, and Clinical Characteristics. Ophthalmology. 2018;125:1929–36.

20. Blankenship GW. Preoperative prognostic factors in diabetic pars plana vitrectomy. Ophthalmology. 1982;89:1246–9.

21. Thompson JT, de Bustros S, Michels RG, Rice TA, Glaser BM. Results of vitrectomy for proliferative diabetic retinopathy. Ophthalmology. 1986;93:1571–4.

22. Ando F, Nagasaka T, Sasano K, Fukumoto K. Factors influencing surgical results in proliferative diabetic retinopathy. German journal of ophthalmology. 1993;2:155–60.

23. Helbig H, Kellner U, Bornfeld N, Foerster MH. [Limits and possibilities of vitreous body surgery in diabetic retinopathy]. Der Ophthalmologe: Zeitschrift der Deutschen Ophthalmologischen Gesellschaft. 1996;93:647–54.

24. Mason JO 3rd, Colagross CT, Haleman T, Fuller JJ, White MF, Feist RM, et al. Visual outcome and risk factors for light perception and no light perception vision after vitrectomy for diabetic retinopathy. Am J Ophthalmol. 2005;140:231–5.

25. Wagner SK, Fu DJ, Faes L, Liu X, Huemer J, Khalid H, et al. Insights into systemic disease through retinal imaging-based oculomics. Transl Vis Sci Technol. 2020;9:6.

26. London A, Benhar I, Schwartz M. The retina as a window to the brain—from eye research to CNS disorders. Nat Rev Neurol. 2013;9:44–53.

27. Zafar S, McCormick J, Giancardo L, Saidha S, Abraham A, Channa R. Retinal Imaging for Neurological Diseases: "A Window into the Brain". Int Ophthalmol Clin. 2019;59:137–54.

28. Cabrera DeBuc D, Somfai GM, Koller A. Retinal microvascular network alterations: potential biomarkers of cerebrovascular and neural diseases. Am J Physiol Heart circulatory Physiol. 2017;312:H201–H12.

29. Ikram MK, de Jong FJ, Bos MJ, Vingerling JR, Hofman A, Koudstaal PJ, et al. Retinal vessel diameters and risk of stroke: the Rotterdam Study. Neurology. 2006;66:1339–43.

30. Ikram MK, De Jong FJ, Van Dijk EJ, Prins ND, Hofman A, Breteler MM, et al. Retinal vessel diameters and cerebral small vessel disease: the Rotterdam Scan Study. Brain : a journal of neurology. 2006;129:182–8.

31. Frost S, Kanagasingam Y, Sohrabi H, Vignarajan J, Bourgeat P, Salvado O, et al. Retinal vascular biomarkers for early detection and monitoring of Alzheimer's disease. Transl Psychiatry. 2013; 3:e233.

32. Cheung CY, Xu D, Cheng C-Y, Sabanayagam C, Tham Y-C, Yu M, et al. A deep-learning system for the assessment of cardiovascular disease risk via the measurement of retinal-vessel calibre. Nat Biomed Eng. 2020:1-11.

33. Ting DS, Peng L, Varadarajan AV, Liu TYA. Novel Retinal Imaging in Assessment of Cardiovascular Risk Factors and Systemic Vascular Diseases. Diabetic Retinopathy and Cardiovascular Disease. 27: Karger Publishers; 2019. p. 106–18.

34. Farrah TE, Webb DJ, Dhaun N. Retinal fingerprints for precision profiling of cardiovascular risk. Nat Rev Cardiol. 2019;16:379–81.

35. Ting DSW, Peng L, Varadarajan AV, Liu TYA. Novel Retinal Imaging in Assessment of Cardiovascular Risk Factors and Systemic Vascular Diseases.

36. Allon R, Aronov M, Belkin M, Maor E, Shechter M, Fabian ID. Retinal Microvascular Signs as Screening and Prognostic Factors for Cardiac Disease: A Systematic Review of Current Evidence. Am J Med. 2020.

37. Bettermann K, Sinha K. Impaired Retinal Vasoreactivity as an Early Marker of Stroke Risk in Diabetes. Stroke Biomarkers: Springer; 2020. p. 245-56.

38. Feke GT, Hyman BT, Stern RA, Pasquale LR. Retinal blood flow in mild cognitive impairment and Alzheimer's disease. Alzheimer's Dementia. 2015;1:144–51.

39. Alber J, Goldfarb D, Thompson LI, Arthur E, Hernandez K, Cheng D, et al. Developing retinal biomarkers for the earliest stages of Alzheimer's disease: What we know, what we don't, and how to move forward. Alzheimer's Dementia. 2020;16:229–43.

40. Anderson B Jr., Saltzman HA. Retinal oxygen utilization measured by hyperbaric blackout. Arch Ophthalmol. 1964;72:792–5.

41. Ames A 3rd. Energy requirements of CNS cells as related to their function and to their vulnerability to ischemia: a commentary based on studies on retina. Can J Physiol Pharmacol. 1992;70: Suppl:S158–64.

42. Vanderkooi JM, Erecińska M, Silver IA. Oxygen in mammalian tissue: methods of measurement and affinities of various reactions. Am J Physiol. 1991;260:C1131–50.

43. Linsenmeier RA. Effects of light and darkness on oxygen distribution and consumption in the cat retina. J Gen Physiol. 1986;88:521–42.

44. Patel SN, Shi A, Wibbelsman TD, Klufas MA. Ultra-widefield retinal imaging: an update on recent advances. Therapeutic Adv Ophthalmol. 2020;12:2515841419899495.

45. Weinreb RN, Aung T, Medeiros FA. The pathophysiology and treatment of glaucoma: a review. JAMA. 2014;311:1901–11.

46. Spaide RF, Klancnik JM Jr., Cooney MJ. Retinal vascular layers imaged by fluorescein angiography and optical coherence tomography angiography. JAMA Ophthalmol. 2015;133:45–50.

47. Dwight JG, Weng CY, Pawlowski ME, Tkaczyk TS. A Dye-Free Analog to Retinal Angiography Using Hyperspectral Unmixing to Retrieve Oxyhemoglobin Abundance. Transl Vis Sci Technol. 2019;8:44.

48. Madhusudhan S, Beare N. Wide-Field Fluorescein Angiography in Wet Age-Related Macular Degeneration. Sci World J. 2014;2014:536161.

49. Spaide RF, Fujimoto JG, Waheed NK. Image artifacts in optical coherence tomography angiography. Retina. 2015;35:2163–80.

50. Holz FG, Bellmann C, Rohrschneider K, Burk RO, Völcker HE. Simultaneous confocal scanning laser fluorescein and indocyanine green angiography. Am J Ophthalmol. 1998;125:227–36.

51. Velez-Montoya ROJ, Mandava N Fluorescein angiography and indocyanine green angiography. In: Yanoff M, Duker JS, eds. Ophthalmology: Expert Consult. Philadelphia, PA: Elsevier-Saunders; 2014:440-7.

52. Lira RP, Oliveira CL, Marques MV, Silva AR, Pessoa Cde C. Adverse reactions of fluorescein angiography: a prospective study. Arquivos brasileiros de oftalmologia. 2007;70:615–8.

53. Yannuzzi LA, Rohrer KT, Tindel LJ, Sobel RS, Costanza MA, Shields W, et al. Fluorescein angiography complication survey. Ophthalmology. 1986;93:611–7.

54. Shao JM, Alimi Y, Conroy D, Bhanot P. Outcomes using indocyanine green angiography with perforator-sparing component separation technique for abdominal wall reconstruction. Surg Endosc. 2020;34:2227–36.

55. Lund-Johansen P. The dye dilution method for measurement of cardiac output. Eur Heart J. 1990;11:6–12.

56. Leevy CM, Smith F, Longueville J, Paumgartner G, Howard MM. Indocyanine green clearance as a test for hepatic function. Evaluation dichromatic ear Densitom JAMA 1967;200:236–40.

57. Hope-Ross M, Yannuzzi LA, Gragoudas ES, Guyer DR, Slakter JS, Sorenson JA, et al. Adverse reactions due to indocyanine green. Ophthalmology. 1994;101:529–33.

58. Shonat RD, Wilson DF, Riva CE, Cranstoun SD. Effect of acute increases in intraocular pressure on intravascular optic nerve head oxygen tension in cats. Investigative Ophthalmol Vis Sci. 1992;33:3174–80.

59. Tsai AG, Johnson PC, Intaglietta M. Oxygen gradients in the microcirculation. Physiol Rev. 2003;83:933–63.

60. Dwight JG, Weng CY, Coffee RE, Pawlowski ME, Tkaczyk TS. Hyperspectral Image Mapping Spectrometry for Retinal Oximetry Measurements in Four Diseased Eyes. Int Ophthalmol Clin. 2016;56:25–38.

61. Rocholz R, Corvi F, Weichsel J, Schmidt S, Staurenghi G OCT Angiography (OCTA) in Retinal Diagnostics. In: Bille JF, editor. High Resolution Imaging in Microscopy and Ophthalmology: New Frontiers in Biomedical Optics. Cham: Springer International Publishing; 2019. p. 135–60.

62. Balaratnasingam C, Inoue M, Ahn S, McCann J, Dhrami-Gavazi E, Yannuzzi LA, et al. Visual Acuity Is Correlated with the Area of the Foveal Avascular Zone in Diabetic Retinopathy and Retinal Vein Occlusion. Ophthalmology. 2016;123:2352–67.

63. Freiberg FJ, Pfau M, Wons J, Wirth MA, Becker MD, Michels S. Optical coherence tomography angiography of the foveal avascular zone in diabetic retinopathy. Graefes Arch Clin Exp Ophthalmol. 2016;254:1051–8.

64. Mihailovic N, Eter N, Alnawaiseh M. [Foveal avascular zone and OCT angiography. An overview of current knowledge]. Der Ophthalmologe: Zeitschrift der Deutschen Ophthalmologischen Gesellschaft. 2019;116:610–6.

65. Ragkousis A, Kozobolis V, Kabanarou S, Bontzos G, Mangouritsas G, Heliopoulos I, et al. Vessel Density around Foveal Avascular Zone as a Potential Imaging Biomarker for Detecting Preclinical Diabetic Retinopathy: An Optical Coherence Tomography Angiography Study. Seminars in Ophthalmology. 2020:1–8.

66. Wons J, Pfau M, Wirth MA, Freiberg FJ, Becker MD, Michels S. Optical Coherence Tomography Angiography of the Foveal Avascular Zone in Retinal Vein Occlusion. Ophthalmologica J Int d'ophtalmologie Int J Ophthalmol Z fur Augenheilkd. 2016;235:195–202.

67. Lee MW, Kim KM, Lim HB, Jo YJ, Kim JY Repeatability of vessel density measurements using optical coherence tomography angiography in retinal diseases. Br J Ophthalmol. 2018.

68. Al-Sheikh M, Tepelus TC, Nazikyan T, Sadda SR. Repeatability of automated vessel density measurements using optical coherence tomography angiography. Br J Ophthalmol. 2017;101:449–52.

69. Chen C-L, Bojikian KD, Xin C, Wen JC, Gupta D, Zhang Q, et al. Repeatability and reproducibility of optic nerve head perfusion measurements using optical coherence tomography angiography. J Biomed Opt. 2016;21:65002.

70. Mihailovic N, Brand C, Lahme L, Schubert F, Bormann E, Eter N, et al. Repeatability, reproducibility and agreement of foveal avascular zone measurements using three different optical coherence tomography angiography devices. PloS ONE. 2018;13: e0206045.

71. Rebhun CB, Moult EM, Ploner SB, Neto CM, Alibhai AY, Schottenhamml J, et al. Analyzing Relative Blood Flow Speeds in Choroidal Neovascularization Using Variable Interscan Time Analysis OCT Angiography. Ophthalmol Retina. 2018;2: 306–19.

72. Campbell JP, Nudleman E, Yang J, Tan O, Chan RVP, Chiang MF, et al. Handheld Optical Coherence Tomography Angiography and Ultra–Wide-Field Optical Coherence Tomography in Retinopathy of Prematurity. JAMA Ophthalmol. 2017;135: 977–81.

73. Yang J, Liu L, Campbell JP, Huang D, Liu G. Handheld optical coherence tomography angiography. Biomed Opt Express. 2017;8:2287–300.

74. Alm A, Bill A. The oxygen supply to the retina. I. Effects of changes in intraocular and arterial blood pressures, and in arterial P O2 and P CO2 on the oxygen tension in the vitreous body of the cat. Acta physiologica Scandinavica. 1972;84:261–74.

75. Stefánsson E, Pedersen DB, Jensen PK, la Cour M, Kiilgaard JF, Bang K, et al. Optic nerve oxygenation. Prog Retinal Eye Res. 2005;24:307–32.

76. Rumsey WL, Vanderkooi JM, Wilson DF. Imaging of phosphorescence: a novel method for measuring oxygen distribution in perfused tissue. Science (New York, NY). 1988;241:1649–51.

77. Quaranta M, Borisov SM, Klimant I. Indicators for optical oxygen sensors. Bioanal Rev. 2012;4:115–57.

78. Lakowicz JR. Principle of fluorescence spectroscopy. Baltimore: Springer; 2006.

79. Holekamp NM, Shui YB, Beebe DC. Vitrectomy surgery increases oxygen exposure to the lens: a possible mechanism for nuclear cataract formation. Am J Ophthalmol. 2005;139:302–10.

80. Williamson TH, Grewal J, Gupta B, Mokete B, Lim M, Fry CH. Measurement of PO2 during vitrectomy for central retinal vein occlusion, a pilot study. Graefes Arch Clin Exp Ophthalmol. 2009;247:1019–23.

81. Nagahara M, Tamaki Y, Araie M, Fujii H. Real-time blood velocity measurements in human retinal vein using the laser speckle phenomenon. Jpn J Ophthalmol. 1999;43:186–95.

82. Riva C, Ross B, Benedek GB. Laser Doppler measurements of blood flow in capillary tubes and retinal arteries. Investigative ophthalmology. 1972;11:936–44.

83. Abegao Pinto L, Vandewalle E, Willekens K, Marques-Neves C, Stalmans I. Ocular pulse amplitude and Doppler waveform analysis in glaucoma patients. Acta ophthalmologica. 2014;92: e280–5.

84. Abegao Pinto L, Vandewalle E, De Clerck E, Marques-Neves C, Stalmans I. Ophthalmic artery Doppler waveform changes associated with increased damage in glaucoma patients. Investigative Ophthalmol Vis Sci. 2012;53:2448–53.

85. Guan K, Hudson C, Flanagan JG. Variability and repeatability of retinal blood flow measurements using the Canon Laser Blood Flowmeter. Microvascul Res. 2003;65:145–51.

86. Haindl R, Trasischker W, Wartak A, Baumann B, Pircher M, Hitzenberger CK. Total retinal blood flow measurement by three beam Doppler optical coherence tomography. Biomed Opt express. 2016;7:287–301.

87. Lee B, Choi W, Liu JJ, Lu CD, Schuman JS, Wollstein G, et al. Cardiac-Gated En Face Doppler Measurement of Retinal Blood Flow Using Swept-Source Optical Coherence Tomography at 100,000 Axial Scans per Second. Investigative Ophthalmol Vis Sci. 2015;56:2522–30.

88. Wang Y, Bower BA, Izatt JA, Tan O, Huang D. In vivo total retinal blood flow measurement by Fourier domain Doppler optical coherence tomography. J Biomed Opt. 2007;12:041215.

89. Dimitrova G, Kato S. Color Doppler imaging of retinal diseases. Survey of ophthalmology. 2010;55:193–214.

90. Harris A, Garzozi HJ, Harris-Izhak M, Shoham N, Holland DR. Color Doppler imaging of central retinal artery in retinopathy of prematurity. Harefuah. 2000;138:812–5. 912

91. Keyser BJ, Flaharty PM, Sergott RC, Brown GC, Lieb WE, Annesley WH, et al. Color Doppler imaging of arterial blood flow in central retinal vein occlusion. Ophthalmology. 1994;101:1357–61.

92. Goodman JW Statistical properties of laser speckle patterns: Springer Verlag; 1984.

93. Fercher AR, Briers JD. Flow visualization by means of single-exposure speckle photography. Opt Commun. 1981;37:326–30.

94. Mangraviti A, Volpin F, Cha J, Cunningham SI, Raje K, Brooke MJ, et al. Intraoperative Laser Speckle Contrast Imaging For Real-Time Visualization of Cerebral Blood Flow in Cerebrovascular Surgery: Results From Pre-Clinical Studies. Scientific reports. 2020;10:7614.

95. Senarathna J, Rege A, Li N, Thakor NV. Laser Speckle Contrast Imaging: theory, instrumentation and applications. IEEE Rev Biomed Eng. 2013;6:99–110.

96. Rege A, Senarathna J, Li N, Thakor NV. Anisotropic processing of laser speckle images improves spatiotemporal resolution. IEEE Trans bio-Med Eng. 2012;59:1272–80.

97. Rege A, Cunningham SI, Liu Y, Raje K, Kalarn S, Brooke MJ, et al. Noninvasive Assessment of Retinal Blood Flow Using a Novel Handheld Laser Speckle Contrast Imager. Transl Vis Sci Technol. 2018;7:7.

98. Briers JD, Fercher AF. Retinal blood-flow visualization by means of laser speckle photography. Investigative Ophthalmol Vis Sci. 1982;22:255–9.

99. Sugiyama T, Araie M, Riva CE, Schmetterer L, Orgul S. Use of laser speckle flowgraphy in ocular blood flow research. Acta Ophthalmologica. 2010;88:723–9.

100. Tsuda S, Kunikata H, Shimura M, Aizawa N, Omodaka K, Shiga Y, et al. Pulse-waveform analysis of normal population using laser speckle flowgraphy. Curr Eye Res. 2014;39:1207–15.

101. Shiga Y, Kunikata H, Aizawa N, Kiyota N, Maiya Y, Yokoyama Y, et al. Optic Nerve Head Blood Flow, as Measured by Laser Speckle Flowgraphy, Is Significantly Reduced in Preperimetric Glaucoma. Curr Eye Res. 2016;41:1447–53.

102. Cho KA, Rege A, Jing Y, Chaurasia A, Guruprasad A, Arthur E, et al. Portable, non-invasive video imaging of retinal blood flow dynamics. Sci Rep. 2020;10:20236.

103. Kalarn S, Cho K-A, Vinnett A, Asanad S, Baroni M, Pottenburgh J, et al. Repeatability and Reproducibility of the XyCAM RI Across Multiple Operators. Investigative Ophthalmol Vis Sci. 2020;61:5321.

104. Rege A, Liu Y, Jing Y, Howarth J, Brooke MJ, Saeedi O. Non-invasive imaging of retinal blood flow with high spatio-temporal resolution. Investigative Ophthalmol Vis Sci. 2017;58:4851.

105. Rege A, Cho K-A, Thompson G, Guruprasad A, Jing Y, Kalarn S, et al. Monitoring blood flow dynamics in retinal arteries and veins using the XyCAM RI. Investigative Ophthalmol Vis Sci. 2019;60:1566.

106. Cho K-A, Wu Y, Lee W-H, O'day J, Rege A, Cabrera DeBuc D. Assessment of Blood Flow Information in Diabetic Eyes using the XyCAM RI. Investigative Ophthalmol Vis Sci. 2020;61:1736.

107. Iwase T, Ra E, Yamamoto K, Kaneko H, Ito Y, Terasaki H. Differences of Retinal Blood Flow Between Arteries and Veins Determined by Laser Speckle Flowgraphy in Healthy Subjects. Medicine. 2015;94:e1256.

108. Rege A, Liu Y, Jing Y, Howarth J, Saeedi O. Non-invasive, non-mydriatic imaging of retinal blood flow over multiple fields of view. Investigative Ophthalmol Vis Sci. 2018;59:5878.

109. Richards LM, Kazmi SM, Davis JL, Olin KE, Dunn AK. Low-cost laser speckle contrast imaging of blood flow using a webcam. Biomed Opt Express. 2013;4:2269–83.

110. Rege A, Murari K, Li N, Thakor NV, editors. Imaging microvascular flow characteristics using laser speckle contrast imaging. Proc 32nd Ann Intl Conf Engr Med Biol Soc (EMBC); 2010; Buenos Aires.

111. Duncan DD, Kirkpatrick SJ. Can laser speckle flowmetry be made a quantitative tool? J Optical Soc Am. 2008;25:2088–94.

112. Wang L, Kwayaki O, Nguyen J, Ogbuokiri E, Murphy O, Caldito N, et al. Microvascular blood floor velocities measured with retinal function imager: intereye correlations in healthy controls and an exploration in multiple sclerosis. Eye Vis. 2018;5:29.

113. Deng Y, Li M, Wang G, Jiang H, Wang J, Li S, et al. The inter-visit variability of retinal blood flow velocity measurements using retinal function imager (RFI). Eye and Vision. 2018;5:31.

114. Flower RW, Kling R. A clinical method for quantification of tissue microvascular blood perfusion in absolute terms [blood-volume/(time.tissue-area)]. Microvascul Res. 2017;114:92–100.

115. Flower RW, Kling R. Observation and characterization of microvascular vasomotion using erythrocyte mediated ICG angiography (EM-ICG-A). Microvasc Res. 2017;113:78–87.

116. Tracey BM, Mayo LN, Le CT, Chen VY, Weichsel J, Renner CY, et al. Measurement of Retinal Microvascular Blood Velocity Using Erythrocyte Mediated Velocimetry. Sci Rep. 2019;9:20178.

117. Wang D, Haytham A, Mayo L, Tao Y, Saeedi O. Automated retinal microvascular velocimetry based on erythrocyte mediated angiography. Biomed Opt Express. 2019;10:3681–97.

118. Geirsdottir A, Palsson O, Hardarson SH, Olafsdottir OB, Kristjansdottir JV, Stefánsson E. Retinal vessel oxygen saturation in healthy individuals. Invest Ophthalmol Vis Sci. 2012;53:5433–42.

119. Hammer M, Vilser W, Riemer T, Schweitzer D. Retinal vessel oximetry-calibration, compensation for vessel diameter and fundus pigmentation, and reproducibility. J Biomed Opt. 2008;13:054015.

120. Lemmens S, Van Eijgen J, Van Keer K, Jacob J, Moylett S, De Groef L, et al. Hyperspectral Imaging and the Retina: Worth the Wave. Transl Vis Sci Technol. 2020;9:9.

121. Beach J, Ning J, Khoobehi B. Oxygen saturation in optic nerve head structures by hyperspectral image analysis. Curr Eye Res. 2007;32:161–70.

122. Stefánsson E, Olafsdottir OB, Einarsdottir AB, Eliasdottir TS, Eysteinsson T, Vehmeijer W, et al. Retinal Oximetry Discovers Novel Biomarkers in Retinal and Brain Diseases. Investigative Ophthalmol Vis Sci. 2017;58:BIO227–BIO233.

123. Hübnerová P, Mlčák P, Šínová I, Karhanová M, Šín M. Current Review of Automatic Retinal Oximetry-A Review. Čes. a slov. Oftal. 2020;76:3–11.

124. Shughoury A, Matthew S, Arciero J, Wurster P, Adjei S, Ciulla T. Retinal oximetry in glaucoma: investigations and findings reviewed. Acta Ophthalmo. 2020;98:559–71.

125. Everdell NL, Styles IB, Calcagni A, Gibson J, Hebden J, Claridge E. Multispectral imaging of the ocular fundus using light emitting diode illumination. Rev Sci Instrum. 2010;81:093706.